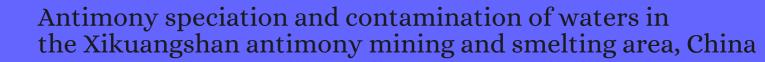
CITATION REPORT List of articles citing



DOI: 10.1007/s10653-010-9284-z Environmental Geochemistry and Health, 2010, 32, 401-13.

Source: https://exaly.com/paper-pdf/47972351/citation-report.pdf

Version: 2024-04-09

This report has been generated based on the citations recorded by exaly.com for the above article. For the latest version of this publication list, visit the link given above.

The third column is the impact factor (IF) of the journal, and the fourth column is the number of citations of the article.

#	Paper	IF	Citations
115	The effect of phosphate application on the mobility of antimony in firing range soils. <i>Science of the Total Environment</i> , 2011 , 409, 2397-403	10.2	44
114	Distribution, speciation and availability of antimony (Sb) in soils and terrestrial plants from an active Sb mining area. <i>Environmental Pollution</i> , 2011 , 159, 2427-34	9.3	160
113	Antimony (Sb) and arsenic (As) in Sb mining impacted paddy soil from Xikuangshan, China: differences in mechanisms controlling soil sequestration and uptake in rice. 2012 , 46, 3155-62		162
112	Application of hyphenated techniques in speciation analysis of arsenic, antimony, and thallium. 2012 , 2012, 902464		26
111	Evolving metalloid signatures in waters draining from a mined orogenic gold deposit, New Zealand. <i>Applied Geochemistry</i> , 2013 , 31, 251-264	3.5	18
110	Removal of antimony (Sb(V)) from Sb mine drainage: biological sulfate reduction and sulfide oxidation-precipitation. 2013 , 146, 799-802		70
109	Fate of Sb(V) and Sb(III) species along a gradient of pH and oxygen concentration in the Carnoul mine waters (Southern France). 2013 , 15, 1536-44		14
108	Multivariate and spatial analysis of heavy metal sources and variations in a large old antimony mine, China. 2013 , 13, 106-116		46
107	Surface complexation modeling and spectroscopic evidence of antimony adsorption on iron-oxide-rich red earth soils. 2013 , 406, 217-24		90
106	Antimony migration trends from a small arms firing range compared to lead, copper, and zinc. <i>Science of the Total Environment</i> , 2013 , 463-464, 222-8	10.2	25
105	Phylogenetic and genome analyses of antimony-oxidizing bacteria isolated from antimony mined soil. 2013 , 76, 76-80		83
104	Simultaneous analysis of SbIII, SbV and TMSb by high performance liquid chromatography-inductively coupled plasma-mass spectrometry detection: application to antimony speciation in soil samples. 2013 , 51, 391-9		23
103	Correlation models between environmental factors and bacterial resistance to antimony and copper. 2013 , 8, e78533		47
102	Bullet on bullet fragmentation profile in soils. <i>Journal of Environmental Management</i> , 2014 , 146, 369-37	'2 7.9	9
101	Antimony uptake, translocation and speciation in rice plants exposed to antimonite and antimonate. <i>Science of the Total Environment</i> , 2014 , 475, 83-9	10.2	94
100	Microbiological reduction of Sb(V) in anoxic freshwater sediments. 2014 , 48, 218-26		83
99	Antimony uptake, efflux and speciation in arsenic hyperaccumulator Pteris vittata. <i>Environmental Pollution</i> , 2014 , 186, 110-4	9.3	40

(2016-2014)

98	Oxidation and mobilization of metallic antimony in aqueous systems with simulated groundwater. 2014 , 132, 16-30		23
97	Arsenic, Antimony, Chromium, and Thallium Speciation in Water and Sediment Samples with the LC-ICP-MS Technique. 2015 , 2015, 171478		16
96	Determination of Carbonate Minerals Responsible for Alkaline Mine Drainage at Xikuangshan Antimony Mine, China: Using Thermodynamic Chemical Equilibrium Model. 2015 , 26, 755-762		10
95	A new method for antimony speciation in plant biomass and nutrient media using anion exchange cartridge. 2015 , 144, 1171-5		7
94	Antimony isotopic composition in river waters affected by ancient mining activity. 2015 , 144, 851-61		21
93	Microbiological oxidation of antimony(III) with oxygen or nitrate by bacteria isolated from contaminated mine sediments. 2015 , 81, 8478-88		61
92	Antimony*. 2015 , 565-579		4
91	Transcriptomic Analysis Reveals Adaptive Responses of an Enterobacteriaceae Strain LSJC7 to Arsenic Exposure. 2016 , 7, 636		17
90	One-Step Extraction of Antimony in Low Temperature from Stibnite Concentrate Using Iron Oxide as Sulfur-Fixing Agent. 2016 , 6, 153		14
89	The role of arbuscular mycorrhizal fungi in plant uptake, fractions, and speciation of antimony. 2016 , 107, 244-250		27
88	Enhanced oxidative and adsorptive capability towards antimony by copper-doping into magnetite magnetic particles. 2016 , 6, 66990-67001		30
87	Analysis of antimony species lessons learnt from more than two decades of environmental research. 2016 , 13, 913		5
86	Treatment of antimony mine drainage: challenges and opportunities with special emphasis on mineral adsorption and sulfate reducing bacteria. 2016 , 73, 2039-51		11
85	Bioaccumulation trends of arsenic and antimony in a freshwater ecosystem affected by mine drainage. 2016 , 13, 149		37
84	Prospective for remediation and purification of wastes from Xikuangshan mine by using Si-based substances. <i>Journal of Environmental Management</i> , 2016 , 172, 77-81	.9	4
83	Growth, photosynthesis, and defense mechanism of antimony (Sb)-contaminated Boehmeria nivea L. 2016 , 23, 7470-81		39
82	Uptake, translocation and transformation of antimony in rice (Oryza sativa L.) seedlings. Environmental Pollution, 2016 , 209, 169-76	.3	42
81	Autotrophic antimonate bio-reduction using hydrogen as the electron donor. 2016 , 88, 467-474		52

80	Comparison of arsenic and antimony biogeochemical behavior in water, soil and tailings from Xikuangshan, China. <i>Science of the Total Environment</i> , 2016 , 539, 97-104	104
79	Mine waste acidic potential and distribution of antimony and arsenic in waters of the Xikuangshan mine, China. <i>Applied Geochemistry</i> , 2017 , 77, 52-61	35
78	Synthesis of Ce(III)-doped FeO magnetic particles for efficient removal of antimony from aqueous solution. <i>Journal of Hazardous Materials</i> , 2017 , 329, 193-204	101
77	Towards finding an efficient sorbent for antimony: comparative investigations on antimony removal properties of potential antimony sorbents. 2017 , 14, 777-784	8
76	Spatial distribution and transport characteristics of heavy metals around an antimony mine area in central China. 2017 , 170, 17-24	84
75	The relative sensitivity of freshwater species to antimony(III): Implications for water quality guidelines and ecological risk assessments. 2017 , 24, 25276-25290	13
74	Prospect for Treating Antimony-Laden Mine Wastewater Using Local Materials. 2017, 36, 379-385	O
73	Bioaccumulation, trophodynamics and ecotoxicity of antimony in environmental freshwater food webs. 2017 , 47, 2208-2258	25
72	Assessment of Industrial Antimony Exposure and Immunologic Function for Workers in Taiwan. 2017 , 14,	6
71	Solid phase microextraction method using a novel polystyrene oleic acid imidazole polymer in micropipette tip of syringe system for speciation and determination of antimony in environmental and food samples. 2018 , 184, 115-121	22
70	Novel Hyper Antimony-Oxidizing Bacteria Isolated from Contaminated Mine Soils in China. 2018 , 35, 713-720	18
69	Coupled S and Sr isotope evidences for elevated arsenic concentrations in groundwater from the world largest antimony mine, Central China. 2018 , 557, 211-221	17
68	Removal of As(V) and Sb(V) in aqueous solution by Mg/Al-layered double hydroxide-incorporated polyethersulfone polymer beads (PES-LDH). <i>Environmental Geochemistry and Health</i> , 2018 , 40, 2119-212 ^{4·7}	12
67	Presence, mobility and bioavailability of toxic metal(oids) in soil, vegetation and water around a Pb-Sb recycling factory (Barcelona, Spain). <i>Environmental Pollution</i> , 2018 , 237, 569-580	15
66	Removal of antimonate from wastewater by dissimilatory bacterial reduction: Role of the coexisting sulfate. <i>Journal of Hazardous Materials</i> , 2018 , 341, 36-45	32
65	Environmental geochemical and spatial/temporal behavior of total and speciation of antimony in typical contaminated aquatic environment from Xikuangshan, China. 2018 , 137, 181-189	36
64	Influence of weak magnetic field and tartrate on the oxidation and sequestration of Sb(III) by zerovalent iron: Batch and semi-continuous flow study. <i>Journal of Hazardous Materials</i> , 2018 , 343, 266-275.8	22
63	Differences in Sb(V) and As(V) adsorption onto a poorly crystalline phyllomanganate (EMnO2): Adsorption kinetics, isotherms, and mechanisms. 2018 , 113, 40-47	36

62	Sequestration of Antimony on Calcite Observed by Time-Resolved Nanoscale Imaging. 2018, 52, 107-11	13	15
61	Pollution and ecological risk assessment of antimony and other heavy metals in soils from the world's largest antimony mine area, China. 2018 , 24, 679-690		11
60	The Release of Antimony from Mine Dump Soils in the Presence and Absence of Forest Litter. 2018 , 15,		9
59	Effects of Antimony Stress on Photosynthesis and Growth of. 2018 , 9, 579		30
58	Comparison of diffusive gradients in thin-films (DGT) and chemical extraction methods for predicting bioavailability of antimony and arsenic to maize. 2018 , 332, 1-9		30
57	Removal of antimonate (Sb(V)) and antimonite (Sb(III)) from aqueous solutions by coagulation-flocculation-sedimentation (CFS): Dependence on influencing factors and insights into removal mechanisms. <i>Science of the Total Environment</i> , 2018 , 644, 1277-1285	10.2	42
56	Bioreduction of Antimonate by Anaerobic Methane Oxidation in a Membrane Biofilm Batch Reactor. 2018 , 52, 8693-8700		43
55	Colorimetrically determining total antimony in contaminated waters and screening for antimony speciation. 2018 , 563, 84-91		6
54	Antimony speciation in the environment: Recent advances in understanding the biogeochemical processes and ecological effects. 2019 , 75, 14-39		160
53	Antimony Causes Mortality and Induces Mutagenesis in the Soil Functional Bacterium Azospirillum brasilense Sp7. 2019 , 230, 1		9
53 52			9
	On-line determination of ultra-trace of antimony species via hydride generation technique using		
52	On-line determination of ultra-trace of antimony species via hydride generation technique using ultrasonic nebulization system coupled to ICP-OES. 2019 , 16, 979-984 Multi-omics reveal various potential antimonate reductases from phylogenetically diverse	9.3	3
52 51	On-line determination of ultra-trace of antimony species via hydride generation technique using ultrasonic nebulization system coupled to ICP-OES. 2019 , 16, 979-984 Multi-omics reveal various potential antimonate reductases from phylogenetically diverse microorganisms. 2019 , 103, 9119-9129 Vegetation type impacts microbial interaction with antimony contaminants in a	9.3	3
52 51 50	On-line determination of ultra-trace of antimony species via hydride generation technique using ultrasonic nebulization system coupled to ICP-OES. 2019 , 16, 979-984 Multi-omics reveal various potential antimonate reductases from phylogenetically diverse microorganisms. 2019 , 103, 9119-9129 Vegetation type impacts microbial interaction with antimony contaminants in a mining-contaminated soil environment. <i>Environmental Pollution</i> , 2019 , 252, 1872-1881 Tissue level distribution of toxic and essential elements during the germination stage of corn seeds		3 13 18
52 51 50 49	On-line determination of ultra-trace of antimony species via hydride generation technique using ultrasonic nebulization system coupled to ICP-OES. 2019 , 16, 979-984 Multi-omics reveal various potential antimonate reductases from phylogenetically diverse microorganisms. 2019 , 103, 9119-9129 Vegetation type impacts microbial interaction with antimony contaminants in a mining-contaminated soil environment. <i>Environmental Pollution</i> , 2019 , 252, 1872-1881 Tissue level distribution of toxic and essential elements during the germination stage of corn seeds (Zea mays, L.) using LA-ICP-MS. <i>Environmental Pollution</i> , 2019 , 252, 657-665 Metal-containing nanoparticles derived from concealed metal deposits: An important source of		3 13 18
52 51 50 49 48	On-line determination of ultra-trace of antimony species via hydride generation technique using ultrasonic nebulization system coupled to ICP-OES. 2019, 16, 979-984 Multi-omics reveal various potential antimonate reductases from phylogenetically diverse microorganisms. 2019, 103, 9119-9129 Vegetation type impacts microbial interaction with antimony contaminants in a mining-contaminated soil environment. Environmental Pollution, 2019, 252, 1872-1881 Tissue level distribution of toxic and essential elements during the germination stage of corn seeds (Zea mays, L.) using LA-ICP-MS. Environmental Pollution, 2019, 252, 657-665 Metal-containing nanoparticles derived from concealed metal deposits: An important source of toxic nanoparticles in aquatic environments. 2019, 224, 726-733 Geochemical behaviors of antimony in mining-affected water environment (Southwest China).	9-3	3 13 18 10

44	Pollution characteristics and ecological risk assessment of 11 unheeded metals in sediments of the Chinese Xiangjiang River. <i>Environmental Geochemistry and Health</i> , 2019 , 41, 1459-1472	4.7	26
43	Mechanism of microbial dissolution and oxidation of antimony in stibnite under ambient conditions. Journal of Hazardous Materials, 2020 , 385, 121561	12.8	23
42	Morpho-physiological traits, gaseous exchange attributes, and phytoremediation potential of jute (Corchorus capsularis L.) grown in different concentrations of copper-contaminated soil. 2020 , 189, 109	9915	52
41	A review of removal technology for antimony in aqueous solution. 2020 , 90, 189-204		58
40	Synthesis of FeO magnetic nanoparticles coated with cationic surfactants and their applications in Sb(V) removal from water. <i>Science of the Total Environment</i> , 2020 , 710, 136302	10.2	31
39	Recycling Antimony(III) by Magnetic Carbon Nanospheres: Turning Waste to Recoverable Catalytic for Synthesis of Esters and Triazoles. 2020 , 8, 469-477		13
38	Influence of sulfur on the mobility of arsenic and antimony during oxic-anoxic cycles: Differences and competition. 2020 , 288, 51-67		14
37	Simultaneous removal of arsenic and antimony from mining wastewater. 2020 , 93, 117-119		4
36	Mutual effects of silver nanoparticles and antimony(III)/(V) co-exposed to Glycine max (L.) Merr. in hydroponic systems: uptake, translocation, physiochemical responses, and potential mechanisms. 2020 , 7, 2691-2707		9
35	Antimony mobility during the early stages of stibnite weathering in tailings at the Beaver Brook Sb deposit, Newfoundland. <i>Applied Geochemistry</i> , 2020 , 115, 104528	3.5	20
34	Multiple effects of nitrate amendment on the transport, transformation and bioavailability of antimony in a paddy soil-rice plant system. 2021 , 100, 90-98		8
33	Transformation of Antimonate at the BiocharBolution Interface. 2021, 1, 2029-2036		2
32	Exposure characteristics of antimony and coexisting arsenic from multi-path exposure in typical antimony mine area. <i>Journal of Environmental Management</i> , 2021 , 289, 112493	7.9	7
31	Reduction of antimony mobility from Sb-rich smelting slag by Shewanella oneidensis: Integrated biosorption and precipitation <i>Journal of Hazardous Materials</i> , 2021 , 426, 127385	12.8	O
30	Clean antimony production from stibnite concentrate with goethite residue co-treatment for zinc, iron, sulfur conservation. 2021 , 313, 127847		O
29	Antimony removal by a magnetic TiO2/SiO2/Fe3O4 nanosphere and influence of model dissolved organic matter. 2021 , 420, 129783		2
28	Effect of Sb on precipitation of biogenic minerals during the reduction of Sb-bearing ferrihydrites. 2021 , 309, 96-111		4
27	Sustainable Applications for Utilizing Antimony Tailing Coarse Aggregate (ATCA) in Concrete: Characteristic of ATCA and Toxicity Risks of Concrete. 2021 , 14,		2

26	Ecological and human health risk assessment of antimony (Sb) in surface and drinking water in China. 2021 , 318, 128514		1
25	Effects of arbuscular mycorrhizal fungi on frond antimony enrichment, morphology, and proteomics in Pteris cretica var. nervosa during antimony phytoremediation. <i>Science of the Total Environment</i> , 2022 , 804, 149904	10.2	1
24	Encyclopedia of Sustainability Science and Technology. 2012 , 4094-4104		1
23	TCEs and environmental research: is the TCEs concept scientifically fruitful?. 2020 , 27, 20565-20570		2
22	A review of the environmental chemical behavior, detection and treatment of antimony. 2021 , 24, 1020	026	2
21	Geochemical Modeling in Environmental and Geological Studies. 2012 , 209-218		
20	Speciation of Inorganic Antimony in Seawater. 2019 , 09, 46-50		
19	Extraction Process of Antimony from Stibnite by Electrothermal Volatilization. 2019 , 665-679		
18	Prokaryotic and Eukaryotic Microbes. 2020 , 149-183		1
17	Individual Water Sources and their Potential Effect on Human and Animal Health in Environmentally Burdened Region. 2020 , 64, 82-94		
16	Antimony contamination and its risk management in complex environmental settings: A review. 2021 , 158, 106908		16
15	Antimony removal from water by pine bark tannin resin: Batch and fixed-bed adsorption. <i>Journal of Environmental Management</i> , 2022 , 302, 114100	7.9	1
14	The leaching of antimony and arsenic by simulated acid rain in three soil types from the world's largest antimony mine area <i>Environmental Geochemistry and Health</i> , 2022 , 1	4.7	О
13	Antimony. 2022 , 23-40		O
12	Antimony redox processes in the environment: A critical review of associated oxidants and reductants <i>Journal of Hazardous Materials</i> , 2022 , 431, 128607	12.8	1
11	Magnetic Ion Imprinted Polymers (MIIPs) for Selective Extraction and Preconcentration of Sb(III) from Environmental Matrices <i>Polymers</i> , 2021 , 14,	4.5	O
10	Antimony Release and Volatilization from Rice Paddy Soils: Field and Microcosm Study. <i>SSRN Electronic Journal</i> ,	1	
9	Stable sulfur and oxygen isotopes of sulfate as tracers of antimony and arsenic pollution sources related to antimony mine activities in an impacted river. <i>Applied Geochemistry</i> , 2022 , 105351	3.5	

8	Uptake, speciation and detoxification of antimonate and antimonite in As-hyperaccumulator Pteris Cretica L. <i>Environmental Pollution</i> , 2022 , 308, 119653	9.3	О
7	Antimony release and volatilization from rice paddy soils: Field and microcosm study. <i>Science of the Total Environment</i> , 2022 , 842, 156631	10.2	О
6	Rhizosphere Microbial Communities and Geochemical Constraining Mechanism of Antimony Mine Waste-Adapted Plants in Southwestern China. 2022 , 10, 1507		О
5	Equilibrium mass-dependent isotope fractionation of antimony between stibnite and Sb secondary minerals: A first-principles study. 2022 , 611, 121115		1
4	Dissimilatory and Cytoplasmic Antimonate Reductions in a Hydrogen-Based Membrane Biofilm Reactor.		O
3	Occurrence, distribution, and migration of antimony in the Zijiang River around a superlarge antimony deposit zone. 2023 , 316, 120520		Ο
2	Antimony (Sb) isotopic signature in water systems from the world largest Sb mine, Central China: Novel insights to trace Sb source and mobilization. 2022 , 130622		0
1	The Legacy of Potential Environmental Soil Contamination in an Antimony Mining Heritage Area. 2023 , 13, 257		1